

# Effect of Coenzyme Q<sub>10</sub> Incorporation on the Characteristics of Nanoliposomes

Shuqin Xia, Shiyong Xu,\* Xiaoming Zhang, and Fang Zhong

School of Food Science and Technology, Southern Yangtze University, Wuxi, 214036, People's Republic of China

Received: September 19, 2006; In Final Form: November 27, 2006

Coenzyme Q<sub>10</sub> (CoQ<sub>10</sub>) is incorporated in nanoliposomes composed of egg yolk phospholipid, cholesterol, and Tween 80. Atomic force microscopy, performed to characterize vesicle surface topology, shows some visible influence of CoQ<sub>10</sub> on the nanoliposomal structure. CoQ<sub>10</sub> incorporation can suppress the increase of the *z*-average diameter of nanoliposomes during storage for 8 months at 4 °C. The liposomal lipid peroxidation caused by Fe(III)/ascorbate is also significantly inhibited. Perturbation of acyl chain motion of lipids due to the presence of CoQ<sub>10</sub> in the bilayer is examined by fluorescence probe diphenyl-hexatriene and Raman spectroscopy. Fluorescence probe studies indicate that CoQ<sub>10</sub> incorporation results in the microviscosity increase of nanoliposomes. The steric structure of nanoliposomes reflected by Raman spectroscopy changes obviously and shows CoQ<sub>10</sub> content dependency. The order parameters for the lateral interaction between chains increase. The *trans* conformation decrease and the *gauche* conformation increase as the weight contents of CoQ<sub>10</sub> incorporation are at 1%, 5%, 10%, and 32.5%. However, the order parameters for the longitudinal interaction in chains was higher than that of pure nanoliposomes as the weight content of CoQ<sub>10</sub> is at 25%. Results suggest that CoQ<sub>10</sub> might intercalate between lipid molecules and perturb the bilayer structure.

## Introduction

Coenzyme Q<sub>10</sub> (CoQ<sub>10</sub>, ubiquinone-10) is an only endogenous synthesized antioxidant existing in all cell membranes of our body.<sup>1</sup> It is essential for production of adenosine triphosphate (ATP), which is the energy source for all living cells. CoQ<sub>10</sub> has been proposed to help treat or possibly even prevent many cardiovascular and neurodegenerative disorders, therefore it has become one of the most popular nutritional supplements.<sup>2</sup> However, because of its higher molecular weight and poor water solubility, CoQ<sub>10</sub> has very low oral bioavailability from the gastrointestinal tract.<sup>3</sup> Several formulation approaches have been adopted to improve in vitro dissolution and absorbability of CoQ<sub>10</sub>, such as using poly(methyl methacrylate) nanoparticles,<sup>4</sup> self-emulsifying delivery systems,<sup>2,3,5</sup> self-microemulsifying delivery systems,<sup>6</sup> nanoemulsified composite system,<sup>7</sup> and liposomes.<sup>8–9</sup>

Liposomes is of particular interest, which are hydrophilic vesicles consisting of one or more concentric bilayers enclosing aqueous compartments.<sup>10–11</sup> The novel delivery system might enhance the shuttling of nutrients with poor water solubility from the intestinal lumen fluids into the enteric cells via bile salt–polar lipid mixed micelles and vesicles.<sup>11</sup> More recent liposome investigations mostly use small vesicles (nanoliposomes) with diameters of the order 50–150 nm, because this size range is a compromise between loading efficiency, stability, and distribution in the organisms.<sup>12–13</sup> In addition, nanoliposomes have the advantages of nanoparticles, which improve the adhesion to and absorption into the intestinal epithelial cells. In this case, the nanoliposomal delivery system might be an effective carrier to improve CoQ<sub>10</sub> absorption.

It has been observed that the content of CoQ<sub>10</sub> incorporated in the nanoliposomes composed of egg yolk phospholipid,

cholesterol, and Tween 80 has obvious effect on the physical and chemical stability of the product during preparation and storage.<sup>14</sup> For understanding the effect of CoQ<sub>10</sub> incorporation on the characteristics of nanoliposomes from molecular level, it is necessary to determine its location and influence on the order of surrounding membrane lipid molecules in liposomal bilayers. The structure of liposomes is very similar to the biological membrane. For illustrating the biological functions of CoQ<sub>10</sub> and some other ubiquinone analogues, many researchers have used phospholipid bilayers as biomembrane model combined with different biophysical techniques to investigate the location of ubiquinone in the membrane. Nevertheless, there is a discrepancy about the interaction of CoQ<sub>10</sub> with liposomal bilayers as well as location and physical state (monomer or aggregate) in the liposome membrane, which probably results from different experimental conditions such as the lipids used, preparation method of liposomes, and CoQ<sub>10</sub> concentrations.<sup>15</sup> Studies based on infrared spectroscopy,<sup>16</sup> nuclear magnetic resonance,<sup>17–18</sup> small-angle X-ray diffraction,<sup>18</sup> differential scanning calorimetry,<sup>18–20</sup> and Raman spectroscopy<sup>20</sup> indicate that the quinone ring of CoQ<sub>10</sub> resides in the midplane regions of the phospholipid bilayer, perhaps even as head to head aggregates. To the contrary, some researchers using fluorescence probe TMA-DPH<sup>15,21</sup> argue that the quinone ring locates near the water–lipid interface. It has also been suggested by several authors that the tail of CoQ<sub>10</sub> are embedded in the hydrophobic slab area of the membrane, with the headgroup just above, but distant from the lipid–water interface.<sup>22</sup> Most of the suggestions aforementioned were obtained from experiments on simple model membrane system formed by synthetic phospholipids such as dipalmitoylphosphatidylcholine (DPPC) and distearoylphosphatidylcholine (DSPC). However, there is little consideration regarding the interaction and location of CoQ<sub>10</sub> in liposomes composed of mixed lipids such as native phospholipid, cholesterol and nonionic surfactant Tween 80. Further,

\* Corresponding author. E-mails: syxu@sytu.edu.cn, sqxia2006@hotmail.com. Telephone: 86-510-85884496. Fax: 86-510-85884496.

the average particle size of liposomes incorporated with CoQ<sub>10</sub> used for experiments has not been given in these reports.

Given the significance of CoQ<sub>10</sub> incorporation for the characteristics of nanoliposomes used as its efficient delivery system, the importance of the interaction between CoQ<sub>10</sub> and the liposomal bilayer component is obvious. Herein we have used atomic force microscopy, fluorescence probe diphenyl-hexatriene, and Raman spectroscopy to investigate the effect of CoQ<sub>10</sub> incorporation on the characteristics of nanoliposomes, especially the hydrocarbon chain structures of membrane lipids. The antioxidant and reducing power of CoQ<sub>10</sub> incorporated in nanoliposomes was also evaluated. On the base of these studies some indication of the distribution of CoQ<sub>10</sub> in the nanoliposome system has been obtained.

## Experimental Section

**Chemicals and Materials.** CoQ<sub>10</sub> material (98.0–101.0% purity) was purchased from Nissin Pharma Inc. (Tokyo, Japan). Standard CoQ<sub>10</sub> (98% purity) was from Sigma Chemical Co. (St. Louis MO). Egg yolk phospholipid (EPL) was purchased from Chemical Reagent Plant of East China Normal University (Shanghai, China). Analytical grade cholesterol (Chol), Tween 80, and ethanol were obtained from China Medicine (Group) Shanghai Chemical Reagent Corp. (Shanghai, China). The fluorescent probe 1,6-diphenyl-1,3,5-hexatriene (DPH, 98% purity) was purchased from Sigma Chemical Co. (St. Louis MO). All other chemicals used were of reagent-grade.

**Preparation of CoQ<sub>10</sub> Nanoliposomes.** The ethanol injection and sonication method<sup>14</sup> was modified slightly in this experiment. Benchtop batches in laboratory were prepared on a 20 mL scale. Different content of CoQ<sub>10</sub> was dissolved in 2 mL of warm ethanol (about 55 °C) together with the lipids composed of EPL, Chol, and Tween 80 (2.5/0.4/1.8, w/w). The ethanol solution was rapidly injected using a syringe as a pump into 20 mL of warm hydration media (0.01 M phosphate buffer solution, PBS, pH 7.4, 0.15 M NaCl) at 55 °C with magnetically stirring. After agitation for 30 min, the ethanol was removed by rotary evaporation (55 °C, 0.1 MPa) to form an aqueous dispersion of liposomes. The final total lipids concentration in the incubations was adjusted to 2.35 mg/mL with deionized water. The prepared liposomal suspension was then submitted to a probing sonication process in an ice bath for 4 min at 350 W with a sequence of 1 s of sonication and 1 s rest using a vibra cell sonicator (VCX500, Sonics & Materials, Inc., 20 kHz) to the desired size. In all cases, the initial turbid liposomal suspension was well translucent after sonication. Following sonication, nanoliposomes were annealed at 4 °C for 12 h. The titanium fragments shed from the probe and any multilamellar vesicles or liposomal aggregates were removed by centrifugation at 11 000g for 30 min at 4 °C. The entire process was carried out in the dark under nitrogen protection to minimize the oxidation and degradation of the lipid mixtures and CoQ<sub>10</sub>. Finally, nanoliposomes were filled into vials (the headspace of the vials was blanketed with nitrogen) and kept in the refrigerator (about 4 °C in the dark).

The incorporation of CoQ<sub>10</sub> nanoliposomes was quantified with Tween 80 solubilization and UV spectrometry followed by an extraction procedure using *n*-pentane, as described in our previous reports.<sup>14</sup> *N*-pentane washing was used to remove CoQ<sub>10</sub> which remained in the aqueous phase. The encapsulation efficiency reached above 95%, which revealed that most of CoQ<sub>10</sub> were incorporated into the liposomal vesicles. In this case, the weight content of CoQ<sub>10</sub> given in this work was almost equal to the actual value of CoQ<sub>10</sub> incorporated into the bilayers.

**Atomic Force Microscopy (AFM) Imaging.** AFM imaging was performed with a Multimode Nanoscope IIIa atomic force microscope from Digital Instruments (Santa Barbara, United States). AFM images were obtained by measurement of the interaction forces between the tip and the sample surface. The experiments were conducted at room temperature (20 °C) and at atmospheric pressure (760 mmHg) operating in tapping mode, in which the space between the tip and the sample is from 10 to 100 Å and the total force is very low. This low force is advantageous to study soft and deformable samples. A triangular silicon tips were used for this analysis. The resonant frequencies of this cantilever were found to be about 300 kHz. Higher resonant frequencies of the cantilever are necessary to minimize the sensitivity to vibrational noise. In order to visualize the liposomes, the noncontact mode is more appropriated because the vesicles are only a little susceptible to load forces applied. Just before the analysis, the samples were diluted in water (1:50) to obtain a less sticky fluid for analyses. Droplets of constant volume (50 μL) were deposited onto a small mica disk with a diameter of 1 cm. After 2 min, the excess of water was removed using paper filter, and the sample chamber was mounted onto the AFM scanner and the measurements were performed and completed within a few minutes to avoid deformation.

**Particle Size Analysis.** The average particle size of the nanoliposomes was determined with a ZetaSizer Nano S (Malvern Instruments Ltd, Malvern, United Kingdom) at a temperature of (25±0.1) °C. The ZetaSizer was modified with a He/Ne laser (λ = 633 nm, Spectra Physics, Mt. View, United States). The intensity of the laser light scattered by the samples was detected at an angle of 90° with a photomultiplier. The undiluted nanoliposome samples of 2 mL were put into a polystyrene latex cell and measured with a refractive index of 1.33. For each specimen 10 autocorrelation functions were analyzed using a cumulant analysis. From this analysis, the *z*-average diameter (*D<sub>z</sub>*) was obtained, which is an approximation of the diameter of the liposomes. The particle size distribution was characterized using the polydispersity index (PDI), which is a measure for the width of the size distribution.

**ζ Potential Measurement.** The ζ potential of the nanoliposomal samples were determined by laser Doppler electrophoretic mobility measurements using the Zeta sizer 2000 (Malvern Instruments Ltd, Malvern, United Kingdom). The samples were diluted to 0.1% (w/w) with PBS before use. All measurements were done at 25 °C, which was controlled with the precision of 0.1 °C. The measurements were repeated 5 times, and the results given were average.

**Microviscosity of Liposomal Bilayer Membranes.** DPH as a fluorescent probe was dissolved in tetrahydrofuran (2×10<sup>-3</sup> mol/L). The DPH solution was diluted to 2×10<sup>-5</sup> mol/L with PBS before use. It was added to the dilute liposome and then incubated at 37 °C for 1 h. The weight ratio of EPL to probe was 2700:1. The microviscosity (η) of liposomes was determined by fluorescence polarization (*P*), which can be calculated according to the following equation:

$$\eta = 2P/(0.46 - P)$$

$$P = (I_{0,0} - GI_{90,0})/(I_{0,0} + GI_{90,0}), \quad G = I_{90,90}/I_{90,0}$$

where *I*<sub>0,0</sub> and *I*<sub>0,90</sub> are the fluorescence intensities of the emitted light polarized parallel and vertical to the exciting light, respectively, and *G* is the grating correction factor.<sup>23</sup> The fluorescence intensities were measured at room temperature (20 °C) with a fluorescence spectrophotometer (650–60, Hvitachi, Ltd., Tokyo, Japan), and excitation and emission wavelengths were 365 and 430 nm, respectively.

**Raman Spectroscopy.** Raman spectra were recorded with a LabRam-1B Raman Micro-spectrometer (Dilor Inc., France) equipped with a Spectra Physics He–Ne laser (typical laser power on the sample: 3 mW at 632.81 nm) at room temperature (20 °C). The slit width was 100  $\mu\text{m}$  and the spectral resolution was approximately 2  $\text{cm}^{-1}$ . The pure nanoliposomes and nanoliposomes containing different weight contents of CoQ<sub>10</sub> (1%, 5%, 10%, 25%, and 32.5%) were prepared as described above and the total weight of lipids was 141 mg/mL. Raman intensities were measured as peak height.

The parameters  $S_L$  and  $S_T$  were calculated as order indices.  $S_L$  refers to the relative intensity of the 2880  $\text{cm}^{-1}$  Raman band that is related to the vibrational coupling between the adjacent chains, and gives a semiquantitative measurement of the lateral interactions between the acyl chains. On the contrary,  $S_T$  refers to the relative intensity of the 1130  $\text{cm}^{-1}$  Raman band that is related to the average number of 'trans' bond in the acyl chain and gives a measure of the order due to intrachain structure. The parameters are normalized so that  $S = 1$  indicates the highest possible order and  $S = 0$  no order (not necessarily the lowest possible).<sup>24</sup> The two parameters might be calculated according to the following equations:<sup>25</sup>

$$S_L = (I_{\text{CH}_2} - 0.7)/1.5, \quad I_{\text{CH}_2} = I_{2890}/I_{2850}$$

$$S_T = (I_{1133}/I_{1087})/1.77$$

**Antioxidant Activity.** The antioxidant power was determined by thiobarbituric acid reactive substance (TBARS), which measures the capacity of CoQ<sub>10</sub> to inhibit the peroxidation of nanoliposomal lipid induced by Fe(III)/ascorbate. The TBARS was detected spectrophotometrically by the method of Rubilar et al.<sup>26</sup> with a slight modification. The nanoliposomes with different contents of CoQ<sub>10</sub> (1 mL, pH 7.4) were mixed with FeCl<sub>3</sub> (1 mL, 400  $\mu\text{mol/L}$ ) and ascorbic acid (1 mL, 1400  $\mu\text{mol/L}$ ). After incubating at 37 °C for 60 min, a solution containing thiobarbituric acid (15% w/v), trichloroacetic acid (0.37% w/v), and hydrochloric acid (1.8% v/v) was added. The system was properly mixed and heated in a boiling water bath for 15 min to promote the formation of a pink pigment resulting from the reaction with malondyaldehyde [(MDA)<sub>2</sub>–TBA]. The sample was cooled, followed by centrifugation at 2500 rpm for 5 min. Clear solution was obtained with this procedure suitable for direct spectrophotometric measurement. The absorbance was measured at 535 nm ( $A_s$ ).  $A_c$  was the absorbance at 535 nm of pure nanoliposomes followed by the above procedure. The inhibition activity (IC) on autooxidation of liposome system induced by Fe(III)/ascorbate was expressed as following equation:

$$\text{IC (\%)} = (A_c - A_s) \times 100/A_c$$

**Reducing Power.** The reducing power of CoQ<sub>10</sub> loaded in nanoliposomes was determined according to the modified method of Dorman et al.<sup>27</sup> The nanoliposomes with different content of CoQ<sub>10</sub> (1 mL, pH 7.4) were mixed with 1 mL of potassium ferricyanide (2.5% w/v); the mixture was incubated at 50 °C for 20 min. At the end of the incubation, 5 mL (20% w/v) of trichloroacetic acid were added to the mixture, which was centrifuged at 3000 rpm for 10 min and filtered. The upper layer of solution (2 mL) was mixed with 2 mL of distilled water and 0.5 mL of FeCl<sub>3</sub> (0.1% w/v). The absorbance was measured at 700 nm. The larger the absorbance is, the higher the reducing power is.

## Results and Discussion

### Effect of CoQ<sub>10</sub> Incorporation on Nanoliposomal Size.

Atomic force microscopy, one of the techniques in the family of scanning probe microscopes with dimensional resolution approaching 1 Å, provides unique possibility for visualizing small liposomes in a natural environment even without sample manipulation.<sup>28</sup> Images of the nanoliposomes were obtained in tapping mode. Tapping mode is known to reduce fractional an adhesive forces that often interfere with imaging of soft samples and therefore is used in this study.<sup>13</sup> Typical amplitude images of the EPL/Chol/Tween 80 nanoliposomes and nanoliposomes containing 25% CoQ<sub>10</sub> are shown in Figure 1. The images resolve individual liposome (spherical particles) on a flat background, which is mica surface. In the pure nanoliposomes (Figure 1a,c), some bigger aggregates formed, whereas in the CoQ<sub>10</sub> nanoliposomes (Figure 1b,d), the vesicles dispersed very well. However the sizes of nanoliposomes observed by AFM sectional analysis were smaller than those obtained from photon correlation spectroscopy. The apparent inconsistent phenomenon has also been observed by some authors<sup>13</sup> who postulate the possible explanations. AFM measure the absorbed vesicles in mica surface; small vesicles have shown to be stable upon absorption, but large vesicles may rupture upon adsorption and are more easily disrupt during AFM scanning.<sup>13</sup> The light scattering technique gives the z-average diameter and the size distribution of vesicles in solution. In any case, the AFM images might reflect the difference of surface topology between pure nanoliposomes and CoQ<sub>10</sub> nanoliposomes to some extent.

Liposomes are thermodynamically unstable, so the vesicles will aggregate, fuse, flocculate and precipitate during storage.<sup>11</sup> It has been observed that the  $D_z$  of CoQ<sub>10</sub>-free nanoliposomes was increased from 117.5 to 260.9 nm after storage at 4 °C for 90 days (3 months), however CoQ<sub>10</sub> incorporation enhanced vesicle resistance to the increase of diameter.<sup>14</sup> The storage time was prolonged to 8 months and the  $D_z$  variations with time are shown in Figure 2a. It was found that the  $D_z$  of pure nanoliposomes increased further to 383.2 nm after 4 months and then almost kept constant from 4 to 6 months followed by decreasing to 327 nm. Seeing through the whole curve as a function of storage time, there existed two dramatic increase steps: the first month and the fourth month. This result can be attributed to the fact that Tween surfactants loaded into nanoliposomes decrease the liposomal energy barrier of aggregation or fusion from the interaction potential.<sup>29</sup>

Compared with the pure nanoliposomes, the  $D_z$  of the nanoliposomes with CoQ<sub>10</sub> changed a little. The increase percent of  $D_z$  after storage for 8 months were 178.3%, 37.78%, 31.18%, 5.53%, and 0.98%, corresponding that the CoQ<sub>10</sub> weight contents were 0%, 10%, 20%, 30%, and 40%, respectively, whereas the polydispersity index values (Figure 2b) demonstrated a small variation during storage. Furthermore the polydispersity index values of nanoliposomes increased with increasing the CoQ<sub>10</sub> content incorporated into the nanoliposomes, suggesting a more heterogeneous liposomal population. The incorporation of different contents of CoQ<sub>10</sub> also did not significantly impact the  $\zeta$  potential of nanoliposomes (Table 1), which indicate that the charges of vesicles are not sufficiently large enough to repel one another and thus overcome the natural tendency to aggregate. It is apparent that the physical stability of EPL/Chol/Tween 80 nanoliposomes during storage could be improved by CoQ<sub>10</sub> incorporation.

**Inhibition of CoQ<sub>10</sub> Incorporation on Peroxidation of Nanoliposomal Lipid.** The antioxidant activity of CoQ<sub>10</sub> in



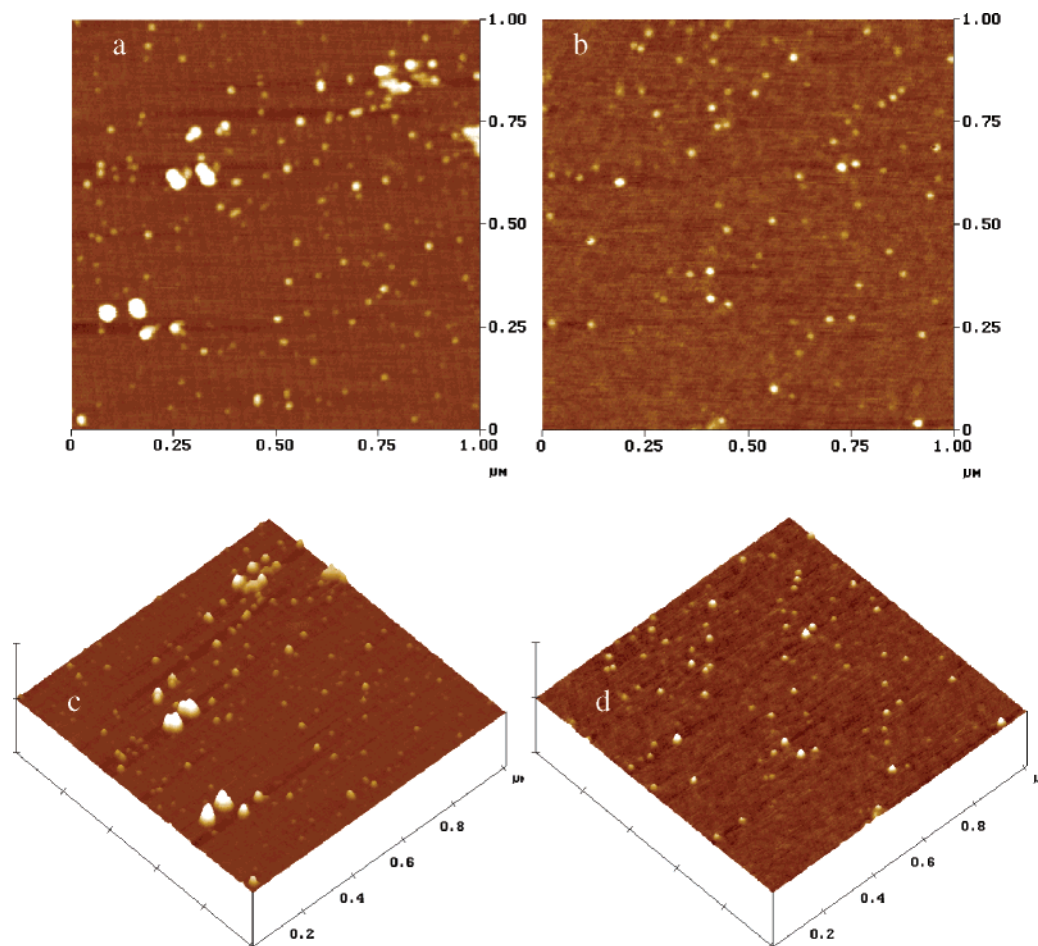


**Figure 1.** Representative atomic force microscopy (AFM) amplitude images of nanoliposomes (bright particles) composed of EPL/Chol/Tween 80 = 2.5/0.4/1.8 (w/w) on mica substrate (dark, flat background) by tapping mode. (a, c) Pure nanoliposomes; (b, d) nanoliposomes containing 25 w% of CoQ<sub>10</sub>.

EPL/Chol/Tween 80 nanoliposome system toward lipid peroxidation induced by Fe(III)/ascorbate mixture was studied. Iron was used as oxidizing agents on the consideration that it is present in human body and is involved in oxidative processes. In the presence of CoQ<sub>10</sub>, the thiobarbituric acid reactive substances (TBARS) production was greatly reduced. Compared with CoQ<sub>10</sub> powder suspension, the TBARS formation was significantly inhibited by CoQ<sub>10</sub> incorporated into nanoliposomes, and the inhibition effect of CoQ<sub>10</sub> was not dose-dependent (Figure 3). This may be due to the fact that the hydrophobic CoQ<sub>10</sub> incorporated in nanoliposomes contacted easily with the unsaturated acyl chains. While the water solubility of CoQ<sub>10</sub> is poor, some CoQ<sub>10</sub> molecules in suspension might absorb into liposomal bilayers and show inhibition on peroxidation of the liposome system induced by Fe(III)/ascorbate to some extent. These reveal that CoQ<sub>10</sub> incorporated in nanoliposomes possess stronger antioxidation ability and could serve as a scavenger of free radicals at the level of membrane. Furthermore, the microenvironment of the media shows obvious influence on the antioxidant ability.

**Fluorescence Probe DPH Analysis.** The characteristics of nanoliposomes are concerned with the fluidity of the membrane lipid. The influence of CoQ<sub>10</sub> incorporation on the membrane structure was evaluated by fluorescence probe DPH that does not perturb the bilayer structure. The majority of the probe molecules is oriented with their long axis aligned parallel to lipid acyl chains but with some population oriented parallel to the membrane surface.<sup>15</sup> Thus, it is able to evaluate the microviscosity around DPH in the liposomal bilayer mem-

branes<sup>23</sup> and reflect average membrane lipid order. It has been shown in our previous studies that the microviscosity is enhanced dramatically once the core material CoQ<sub>10</sub> is incorporated into bilayers and then increased slowly with the CoQ<sub>10</sub> content ranging from 5 to 40%.<sup>14</sup> In order to investigate whether a small amount of CoQ<sub>10</sub> incorporation had this ability, the CoQ<sub>10</sub> content in nanoliposomes was decreased to 1%. The result (Figure 4) indicates that the microviscosity in nanoliposomes increases to a smaller extent as compared to pure nanoliposomes.

The fluorescence probe DPH is strongly hydrophobic, which produces an intense fluorescence emission when incorporated in hydrophobic membrane region.<sup>30</sup> CoQ<sub>10</sub> incorporation into nanoliposomes has also been shown quench the fluorescence of DPH probe with the CoQ<sub>10</sub> content in the range from 5% to 40%.<sup>14</sup> Similar fluorescence quenching was observed if lowering the content of CoQ<sub>10</sub> to 1% (Figure 4). This suggests that the quenching group of the CoQ<sub>10</sub> molecules, presumably the benzoquinone ring, is accessible to the fluorescent group of the probe, even if the content is lowered to 1%.

The increase rates of the  $F_0/F$  and microviscosity at CoQ<sub>10</sub> content below 5% were higher. The effects were less pronounced when increasing the CoQ<sub>10</sub> content. These phenomena reveal that CoQ<sub>10</sub> at higher concentrations would accumulate within the hydrophobic midplane region of the membrane, which probably does not come into contact with the membrane zone occupied by DPH molecules, therefore causing also less perturbation change of the membrane lipid arrangement. Our results are in agreement with the reports by Skowronek et al.<sup>21</sup>

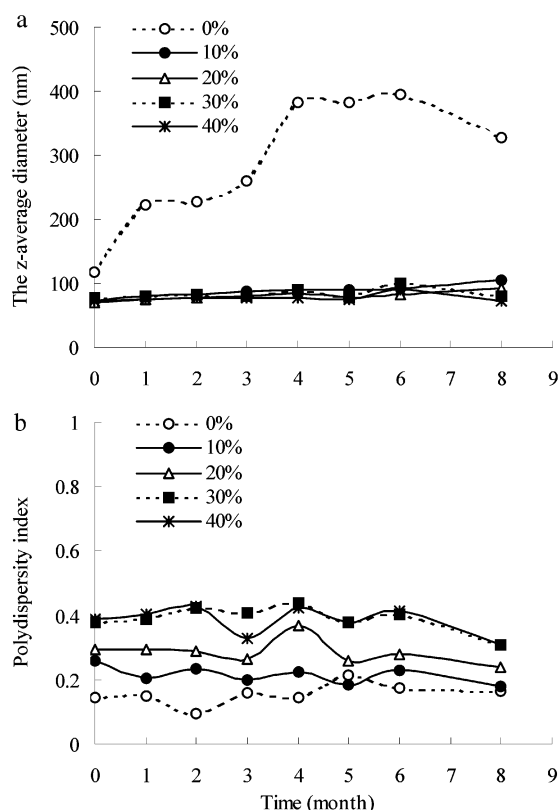


**Figure 2.** The z-average diameter (a) and polydispersity index value (b) variation of pure nanoliposomes and nanoliposomes with different weight contents of CoQ<sub>10</sub> during storage at 4 °C in the dark as a function of time. The weight ratio of EPL/Chol/Tween 80 was 2.5:0.4:1.8. The weight contents of CoQ<sub>10</sub> incorporation were 0%, 10%, 20%, 30%, and 40%.

**TABLE 1: The Values of  $\zeta$  Potential of Pure Nanoliposomes and Nanoliposomes Containing Different Weight Contents of CoQ<sub>10</sub>**

CoQ <sub>10</sub> content (%, w/w) <sup>a</sup>	0	10	20	30	40
$\zeta$ potential (mV)	$6.2 \pm 0.9^b$	$4.3 \pm 1.7$	$1.6 \pm 1.3$	$3.9 \pm 0.2$	$4.3 \pm 1.4$

<sup>a</sup> EPL/Chol/Tween 80 (2.5:0.4:1.8, w/w) nanoliposomes. The content is the weight percentage of CoQ<sub>10</sub> against the lipids. <sup>b</sup> Data represent means  $\pm$  standard deviation from five determination.

The anisotropy value is also used as an index to evaluate the extent of probe motion during its excited lifetime. A high anisotropy value means that the motion is limited by an ordered environment of the probe. Their reports had suggested that CoQ<sub>10</sub> strongly induce ordering of egg yolk lecithin membrane structure, which was attributed to methoxyl groups of the quinone rings.<sup>21</sup> But the CoQ<sub>10</sub> content in their studies varied between 1 mol % to 10 mol %, and higher CoQ<sub>10</sub> content in liposomes was not given further consideration. In addition, they had found that CoQ<sub>10</sub> showed very small ordering effect on DPPC bilayers, which was different from the results in unsaturated lipids.

**Raman Analysis.** Since CoQ<sub>10</sub> might partly intercalate between lipid molecules and decrease the fluidity of bilayers showed by fluorescence probe technique, Raman spectroscopy was used to investigate the effect of CoQ<sub>10</sub> incorporation at some concentrations on the order parameters of nanoliposomes. Raman spectroscopy has been proved to be a powerful, noninvasive and complementary technique to detect changes in the environment of lipid hydrocarbon chains when other molecules are intercalated into lipid bilayers.<sup>24</sup> The change of

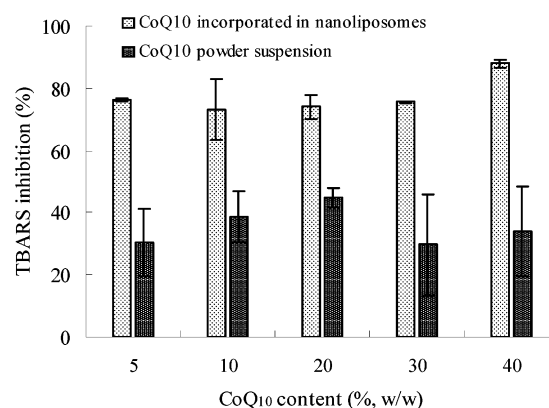


**Figure 3.** Effect of CoQ<sub>10</sub> incorporated in nanoliposomes and CoQ<sub>10</sub> powder suspension on the inhibition of thiobarbituric acid reactive substances (TBARS) formation in nanoliposome system induced by Fe(III)/ascorbate. Each point represents the mean  $\pm$  standard deviation ( $n = 3$ ).

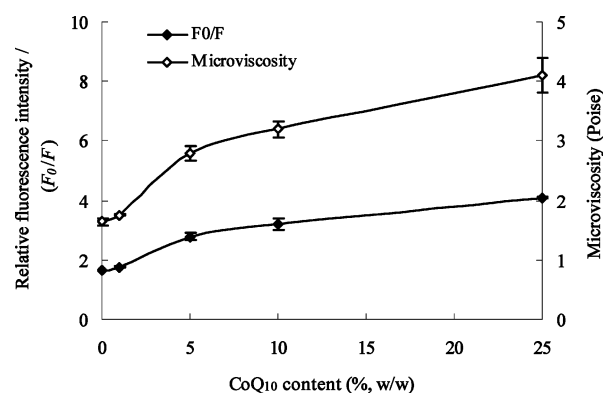


**Figure 4.** Fluorescence quenching ( $F_0/F$ ) of DPH probes and microviscosity change of EPL/Chol/Tween 80 (2.5:0.4:1.8, w/w) nanoliposomes by increasing the weight contents of incorporated CoQ<sub>10</sub>.  $F_0$  is referred to the fluorescence intensity of pure nanoliposomes;  $F$  is referred to the fluorescence intensity of nanoliposomes with different content of CoQ<sub>10</sub>. Each point represents the mean  $\pm$  standard deviation ( $n = 3$ ).

*trans* and *gauche* conformations by hydrocarbon chains of lipids, and that of the order parameters for the longitudinal interaction within chains and for the lateral interaction between chains indicate the character of structural changes of liposomes.<sup>31</sup> Herein, the structural changes of EPL/Chol/Tween 80 nanoliposomes by CoQ<sub>10</sub> incorporation in a dose-dependent way were investigated by observing the change of the important Raman bands in the regions 2800–3000, 1000–1200, and 1200–1800 cm<sup>-1</sup>. By plotting the intensities of some characteristic Raman bands, sharp changes were observed in correspondence to the structural changes in the liposome and particularly in their inner hydrophobic core.

The Raman spectra in the region from 2800 to 3000 cm<sup>-1</sup> of pure nanoliposomes and nanoliposomes containing 1, 5, 10, 25, and 32.5% (w/w) CoQ<sub>10</sub> are presented in Figure 5. These spectra showed that all of the spectral features of the lipid molecules were retained when CoQ<sub>10</sub> were present in weight contents of up to 32.5% at room temperature. The strong bands located at about 2850 and 2890 cm<sup>-1</sup> correspond to the symmetric  $\nu_s$  (CH<sub>2</sub>) and antisymmetric  $\nu_{as}$  (CH<sub>2</sub>) C–H stretching vibrations of the methylene groups of the acyl chains of lipids, respectively. These two bands are quite sensitive to the change of their conformation and widely used to study the structure of lipid bilayers of membrane.<sup>32</sup> When different contents of CoQ<sub>10</sub> were incorporated into nanoliposomes, the latter band were located at the following wavelengths: 2886 cm<sup>-1</sup> (0%); 2883 cm<sup>-1</sup> (1%);

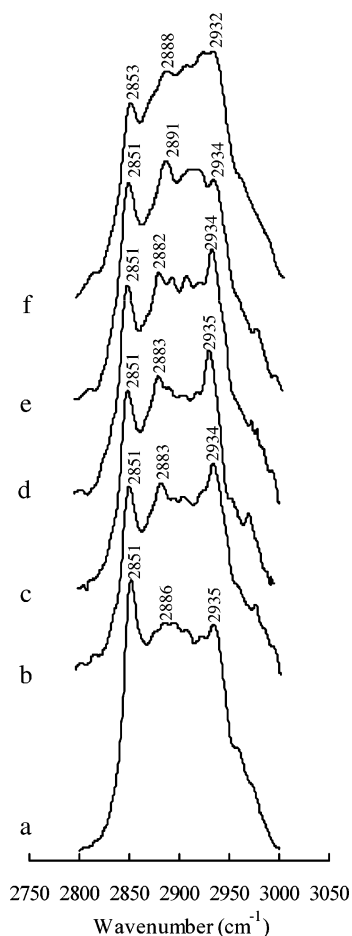


**Figure 5.** Raman spectra in the range between 2800 and 3000  $\text{cm}^{-1}$  of pure nanoliposomes (a) and nanoliposomes with increasing weight contents of CoQ<sub>10</sub>: 1% (b), 5% (c), 10% (d), 25% (e), and 32.5% (f).

2883  $\text{cm}^{-1}$  (5%); 2882  $\text{cm}^{-1}$  (10%), 2891  $\text{cm}^{-1}$  (25%), and 2888  $\text{cm}^{-1}$  (32.5%). The order parameters reflecting the state of lateral packing of the nanoliposomes are summarized in Table 2. The data showed that the incorporation of very small amounts of CoQ<sub>10</sub> (1% and 5%, w/w) caused a noticeable increase in  $S_L$  for the lateral interaction between chains, suggesting the lateral packing tighten. The increase of  $S_L$  was not profound as further increasing the CoQ<sub>10</sub> concentrations to 10% and 25% (w/w). The change tendency was co-incident with fluorescence polarization measurements, which exhibited a significant decrease in the rotational motion of DPH in nanoliposomes containing CoQ<sub>10</sub> at the concentrations below 5%. Nevertheless, the  $S_L$  increased significantly if further increasing the CoQ<sub>10</sub> content (32.5% w/w).

The bands at 1054  $\text{cm}^{-1}$  and 1133  $\text{cm}^{-1}$  correspond to the *all-trans* bond-stretching vibration of the C–C skeleton and the band at 1086  $\text{cm}^{-1}$  corresponds to *gauche* rotamers. The changes of three lines are observed in Figure 6. As different contents of CoQ<sub>10</sub> were incorporated into nanoliposomes, the three bands shifted at the following wavelengths: 1055, 1088, and 1132

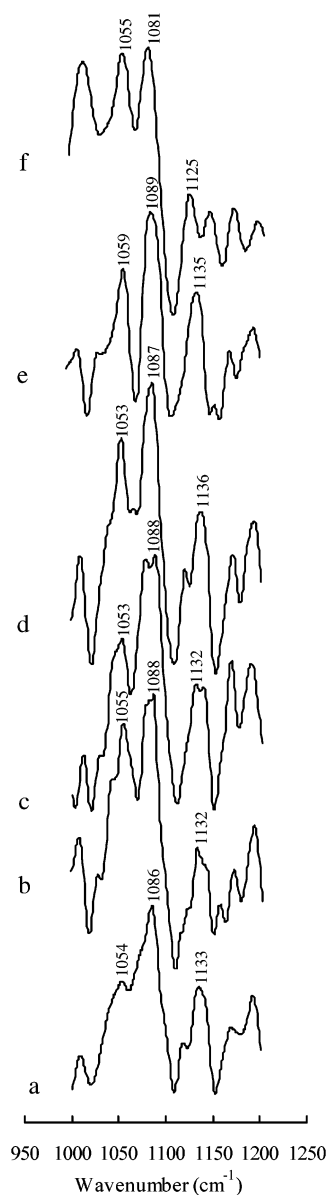


**Figure 6.** Raman spectra in the range between 1000 and 1200  $\text{cm}^{-1}$  of pure nanoliposomes (a) and nanoliposomes with increasing weight contents of CoQ<sub>10</sub>: 1% (b), 5% (c), 10% (d), 25% (e), and 32.5% (f).

$\text{cm}^{-1}$  (1%); 1053, 1088, and  $1132 \text{ cm}^{-1}$  (5%); 1033, 1087, and  $1136 \text{ cm}^{-1}$  (10%); 1059, 1089, and  $1135 \text{ cm}^{-1}$  (25%); 1055, 1081, and  $1125 \text{ cm}^{-1}$  (32.5%). The more *all-trans* bonds there are, the larger the longitudinal order parameter is. For *gauche* rotamers, the result is the opposite. Therefore, the ratio of the intensity of line at around  $1133 \text{ cm}^{-1}$  to that of the line at around  $1086 \text{ cm}^{-1}$  reflected the degree of the longitudinal order of liposomes.<sup>31</sup>  $S_T$  decreased dramatically from 0.30 to 0.19 as the CoQ<sub>10</sub> content increased from 0% (w/w) to 1% (w/w), this might be interpreted as the quinones having a disordering effect upon the lipid acyl chains. While  $S_T$  increased as further increasing

**TABLE 2: Order Parameters of Nanoliposomes Containing Different Weight Contents of CoQ<sub>10</sub> and Variation Percent as Deduced from Raman Spectra**

CoQ <sub>10</sub> content (%, w/w)	0	1	5	10	25	32.5
$S_L$	0.0956	0.2147	0.2487	0.2391	0.2534	0.3090
$(S_L - S_{L,0})/S_{L,0}$	—	124.58%	160.15%	150.10%	165.06%	223.22%
$S_T$	0.3038	0.1944	0.2605	0.2756	0.3445	0.2144
$(S_T - S_{T,0})/S_{T,0}$	—	−36.02%	−14.26%	−9.3%	13.37%	−29.43%
$I_{1658}/I_{1444}$	0.9132	1.1949	1.2771	1.6402	2.5299	2.5113

**TABLE 3: The Reducing Power of CoQ<sub>10</sub> Incorporated in Nanoliposomes**

CoQ <sub>10</sub> content % (w/w) <sup>a</sup>	5	10	20	30	40
A <sub>700 nm</sub>	0.014 ± 0.003 <sup>b</sup>	0.048 ± 0.003	0.088 ± 0.007	0.116 ± 0.010	0.186 ± 0.028

<sup>a</sup> EPL/Chol/Tween 80 (2.5:0.4:1.8, w/w) nanoliposomes. The content is the weight percentage of CoQ<sub>10</sub> against the lipids. <sup>b</sup> Data represent means ± standard deviation from three determination.

the CoQ<sub>10</sub> content (Table 2). It was interesting to find that the longitudinal order parameter was greatly higher than that of the pure nanoliposomes as the CoQ<sub>10</sub> content was up to 25% (w/w), suggesting *all-trans* bonds increased and *gauche* rotamers decreased. Likewise, the *S<sub>T</sub>* showed significant decrease when increasing the CoQ<sub>10</sub> content to 32.5% (w/w).

The increase in *S<sub>L</sub>* and the decrease in *S<sub>T</sub>* even in the presence of small CoQ<sub>10</sub> content, confirmed the marked sensitivity of nanoliposomes to the presence of CoQ<sub>10</sub>. However measurement of the intensity ratios in both the C–H and C–C stretching frequencies did not show any evidence for structural perturbation of the hydrocarbon chains due to the presence of CoQ<sub>10</sub> at 1, 3, and 5 mol % when using membrane model composed of DPPC,<sup>32</sup> which is in apparent contraction to our observation.

The Raman spectra in the region from 1200 to 1750 cm<sup>−1</sup> attracted our interest and are given in Figure 7. This region of the spectrum also contains most of the strongly resonating bands of CoQ<sub>10</sub>,<sup>32</sup> as shown in Figure 7g. The C=O stretching mode of lipids as well as the C=O stretching bands due to carbonyl group of the quinone ring of CoQ<sub>10</sub> have been studied. The C=O groups of the quinone ring of CoQ<sub>10</sub> lies at about 1663 cm<sup>−1</sup>. Additionally, the Raman band at 1658 cm<sup>−1</sup> is also attributed to the *cis*-C=C bond of lipids,<sup>33</sup> because the nanoliposomal bilayers are composed of lipids which containing unsaturated fatty acids (Figure 7a). The intensities of the band were relatively high compared with the C=O band of the phospholipid centered at around 1733 cm<sup>−1</sup>. The C=O stretching mode band of lipid indicates that CoQ<sub>10</sub> did not have an important interaction with the C=O group of lipids, corresponding to observed previously by FT–IR techniques.<sup>16</sup> Significant variations of the band at around 1658 cm<sup>−1</sup> were observed as increasing the CoQ<sub>10</sub> contents. The relative intensity change of the Raman line at about 1658 cm<sup>−1</sup> normalized to the C–C Raman band<sup>32</sup> at about 1444 cm<sup>−1</sup> in nanoliposomal is shown in Table 2, which is lower as compared to that of pure CoQ<sub>10</sub> (*I*<sub>1663</sub>/*I*<sub>1443</sub> = 4.0927). The changes observed here might reveal the changes in acyl chain packing and conformational order, which arise from the incorporation of CoQ<sub>10</sub> into the nanoliposomal bilayers.

Jain and Wu<sup>34</sup> have found that at least four types of effects by foreign lipid-soluble compounds on the transition of dipalmitoyl lecithin bilayer could be generally observed by differential scanning calorimetry, each one corresponded to a localization of the additive in the bilayer. However CoQ<sub>10</sub> arrangement obtained from Raman analysis is not included in these four types, this might be explained that CoQ<sub>10</sub> in the straight-chain trans configuration has a length of 56 Å, i.e., greater than the thickness of a phospholipid bilayer.<sup>16</sup> The quinone rings of longer-chain ubiquinones are normally buried deeply in the bilayer, but the high curvature on the inside of small vesicles allows the rings to come closer to the surface.<sup>17</sup> Since the lipid packing was significantly perturbed by CoQ<sub>10</sub> incorporation and content-dependent, it was likely to conclude that the side-chain of CoQ<sub>10</sub> at least partly located parallel to the lipid hydrocarbon chains and the methyl substituents of quinone rings played the role. This model explains why the CoQ<sub>10</sub> molecules incorporated into nanoliposomes catalyzing ferricyanide reduction in the bulk phase (Table 3). Ferricyanide is an oxidizing agent impermeable through lipid bilayers and

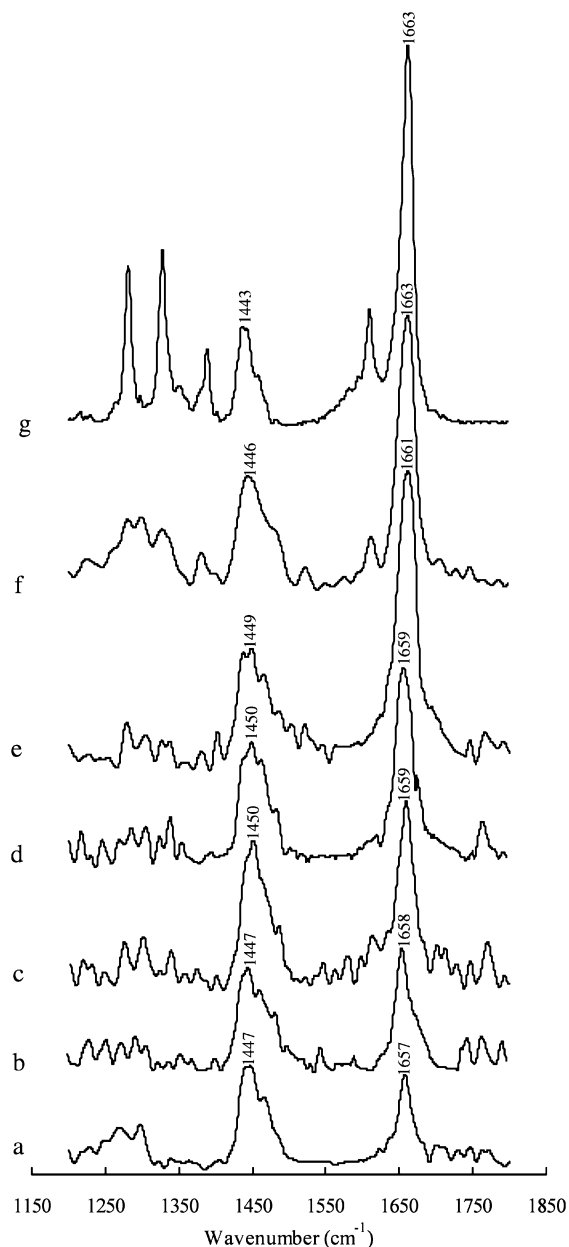


**Figure 7.** Raman spectra between 1200 cm<sup>−1</sup> and 1800 cm<sup>−1</sup> of pure nanoliposomes (a) and nanoliposomes with increasing weight contents of CoQ<sub>10</sub>: 1% (b), 5% (c), 10% (d), 25% (e), 32.5% (f), and pure CoQ<sub>10</sub> (g).

membranes, and therefore extensively used to assess the exposition of redox groups to the aqueous medium.<sup>32</sup> The efficiently reducing power of CoQ<sub>10</sub> incorporated into nanoliposomes supported that at least part of CoQ<sub>10</sub> has the possibility of diffusion toward the membrane/water interface regions of the liposomal bilayers where the redox changes take place. It was also found that the reducing power increased with the increase of CoQ<sub>10</sub> content.

## Conclusions

It seems reasonable to conclude that CoQ<sub>10</sub> might associate with particular lipids, adjust bilayer fluidity and somewhat give



rise to a more ordered arrangement of lipids molecules in nanoliposomes composed of EPL, cholesterol, and Tween 80 as a delivery system. Furthermore, the extent of the effect depends on the content of CoQ<sub>10</sub> incorporation. It would be interesting to extract from these observations some information concerning the molecular location and organization of CoQ<sub>10</sub> in nanoliposomal bilayers. In any case, at least part of the quinone rings of CoQ<sub>10</sub> might locate in the hydrophobic slab area of the bilayer, since this is the region in which insertion of hydrophobic compounds would disturb the packing of the lipid molecules. The experimental data also imply that the biological functions and physiological effects of CoQ<sub>10</sub> could arise partially from their capability to modify to some extent the biomembrane bilayer structure.

**Acknowledgment.** The authors would like to acknowledge the financial support from the Graduate Student Innovation Project (Jiangsu, China).

## References and Notes

- (1) Bentinger, M.; Dallner, G.; Chojnacki, T.; Swiezewska, E. *Free. Radical. Biol. Med.* **2003**, *34*, 563.
- (2) Palamakula, A. PhD Dissertation, Texas Tech University, Lubbock, TX, 2004.
- (3) Kommuru, T. R.; Gurley, B.; Khan, M. A.; Reddy, I. K. *Int. J. Pharm.* **2001**, *212*, 233.
- (4) Kwon, S. S.; Nam, Y. S.; Lee, J. S.; Ku, B. S.; Han, S. H.; Lee, J. Y.; Chang, I. S. *Colloids Surf. A* **2002**, *210*, 95.
- (5) Palamakula, A.; Khan, M. A. *Int. J. Pharm.* **2004**, *273*, 63.
- (6) Kang, B. K.; Lee, J. S.; Chon, S. K.; Jeong, S. Y.; Yuk, S. H.; Khang, G.; Lee, H. B.; Cho, S. H. *Int. J. Pharm.* **2004**, *274*, 65.
- (7) Carli, F.; Chiellini, E. E.; Bellich, B.; Macchiavelli, S.; Cadelli, G. *Int. J. Pharm.* **2005**, *291*, 113.
- (8) Crestanello, J. A.; Doliba, N. M.; Natalia, M. D.; Babsky, A. M.; Niborri, K.; Osbakken, M. D.; Whitman, G. J. R. *J. Surg. Res.* **2002**, *102*, 221.
- (9) Enzmann, F.; Lachmann, B. U.S. 20020155151, 2002.
- (10) Xia, S.; Xu, S. *Food Res. Int.* **2005**, *38*, 289.
- (11) Keller, B. C. *Trends Food Sci. Technol.* **2001**, *12*, 25.
- (12) Sulkowski, W. W.; Pentak, D.; Nowak, K.; Sulkowska, A. *J. Mol. Struct.* **2005**, 737.
- (13) Liang, X.; Mao, G.; Ng, K. Y. S. *J. Colloid Interface Sci.* **2004**, *278*, 53.
- (14) Xia, S.; Xu, S.; Zhang, X. *J. Agric. Food. Chem.* **2006**, *54*, 6358.
- (15) Jemiot-Rzeminska, M.; Kruk, J.; Skowronek, M.; Strzatka, K. *Chem. Phys. Lipids* **1996**, *79*, 55.
- (16) Aranda, F. J.; Villalain, J.; Gomez-Fernandez, J. C. *Biochim. Biophys. Acta Biomembr.* **1986**, *861*, 25.
- (17) Kingsley, P. B.; Feigenson, G. W. *Biochim. Biophys. Acta Bioenerge.* **1981**, *635*, 602.
- (18) Gomez-Fernandez, J. C.; Llamas, M. A.; Aranda, F. J. *Eur. J. Biochem.* **1999**, *259*, 739.
- (19) Jemiot-Rzeminska, M.; Mysliwa-Kurziel, B.; Strzatka, K. *Chem. Phys. Lipids* **2002**, *114*, 169.
- (20) Roche, Y.; Peretti, P.; Bernard, S. *Thermochim. Acta* **2006**, *447*, 81.
- (21) Skowronek, M.; Jemiot-Rzeminska, M.; Kruk, J.; Strzatka, K. *Biochim. Biophys. Acta Biomembr.* **1996**, *1280*, 115.
- (22) Afri, M.; Ehrenberg, B.; Talmon, Y.; Schmidt, J.; Cohen, Y.; Frimer, A. A. *Chem. Phys. Lipids* **2004**, *131*, 107.
- (23) Imura, T.; Sakai, H.; Yamauchi, H.; Kaise, C.; Kozawa, K.; Yokoyama, S.; Abe, M. *Colloids Surf. B* **2001**, *20*, 1.
- (24) Bonora, S.; Torreggiani, A.; Fini, G. *Thermochim. Acta* **2003**, *408*, 55.
- (25) Gaber, B. P.; Peticolas, W. L. *Biochem. Biophys. Acta Biomembr.* **1977**, *465*, 260.
- (26) Rubilar, M.; Pinelo, M.; Ihl, M.; Scheuermann, E.; Sineiro, J.; Nunez, M. J. *J. Agric. Food. Chem.* **2006**, *54*, 59.
- (27) Dorman, H. J. D.; Kosar, M.; Kahlos, K.; Holm, Y.; Hiltunen, R. *J. Agric. Food. Chem.* **2003**, *51*, 4563.
- (28) Ruozzi, B.; Tosi, G.; Forni, F.; Fresta, M.; Vandelli, M. A. *Eur. J. Pharm. Sci.* **2005**, *25*, 81.
- (29) Tasi, L. M.; Liu, D. Z.; Chen, W. Y. *Colloids Surf. A* **2003**, *213*, 7.
- (30) Pandey, B. N.; Mishra, K. P. *Radiat. Phys. Chem.* **1999**, *54*, 481.
- (31) Xu, Y.; Yang, H.; Yan, Y.; Zhang, Z. *J. Photochem. Photobiol. B: Biology* **1998**, *45*, 179.
- (32) Lenaz, G. Thermal characteristics of coenzyme Q and its interaction with model membrane systems. *Coenzyme Q: Biochemistry, Bioenergetics and Clinical Application of Ubiquinone*; John Wiley & Sons Ltd.: New York, 1985; p 107.
- (33) Sailer, K.; Viaggi, S.; Nüsse, M. *Biochem. Biophys. Acta Biomembr.* **1997**, *1329*, 259.
- (34) Jain, M. K.; Wu, N. Y. *J. Membr. Biol.* **1977**, *34*, 157.